Theor Appl Climatol (2011) 106:45–53
DOI 10.1007/s00704-011-0419-7

ORIGINAL PAPER

Early summer temperature reconstruction in the eastern Tibetan plateau since AD 1440 using tree-ring width of *Sabina tibetica*

Hai-Feng Zhu · Xue-Mei Shao · Zhi-Yong Yin · Lei Huang

Received: 26 September 2010 / Accepted: 8 February 2011 / Published online: 22 February 2011

Abstract Long climate records are scarce on the Tibetan Plateau for understanding the climate variability on long-term context. Here we presented an early summer (May–June) temperature reconstruction since AD 1440 for Qamdo area using tree rings of *Sabina tibetica*. The reconstruction accounted for 64% of the variance in the instrumental record. It showed warm periods during 1501–1514, 1528–1538, 1598–1609, 1624–1636, 1650–1668, 1695–1705, 1752–1762, 1794–1804, 1878–1890, 1909–1921, 1938–1949, and 1979–1991. Cool early summer occurred during 1440–1454, 1482–1500, 1515–1527, 1576–1597, 1610–1621, 1669–1679, 1706–1716, 1782–1793, 1863–1873, 1894–1908, and 1922–1937. Comparison with other proxy or meteorological records suggested that there is obvious spatial variability in the May–June temperature variations along the eastern margin of the Tibetan Plateau.

H.-F. Zhu (✉)
Key Laboratory of Tibetan Environment Changes and Land Surface Processes, Institute of Tibetan Plateau Research, Chinese Academy of Sciences,
Beijing 100085, China
e-mail: zhuhf@igsnrr.ac.cn
e-mail: zhuhf05@gmail.com

H.-F. Zhu · X.-M. Shao
Institute of Geographic Sciences and Natural Resources Research, Chinese Academy of Sciences,
Beijing 100101, China

X.-M. Shao
e-mail: shaoxm@igsnrr.ac.cn

Z.-Y. Yin
Department of Marine Science and Environmental Studies, University of San Diego,
San Diego, CA 92110, USA
e-mail: zyin@sandiego.edu

L. Huang
National Climate Center,
Beijing 100081, China
e-mail: huanglei@cma.gov.cn

1 Introduction

The Tibetan Plateau (TP), with an area of about 2,300,000 km^2, influences the large-scale circulation system, such as the Asian Monsoon, through its thermal effect (He et al. 1987; Li and Yanai 1996; Wu and Zhang 1998; Zhou et al. 2009). It is important to understand the climate variability over the TP. However, most meteorological records on the TP are of short length (less than 60 years) and distributed sparsely, limiting the study of the climate variability on long-term timescale. An enhanced understanding of past climatic variability on the TP must rely on climatic proxies.

Tree rings, as an annually resolved proxy record, have been increasingly used to reconstruct past climate changes on the TP (e.g., Bräuning and Mantwill 2004; Gou et al. 2008; Liang and Eckstein 2009; Liang et al. 2008; Liu et al. 2007; Liu et al. 2006; Shao et al. 2005; Shi et al. 2010; Wang et al. 2009; Yang et al. 2009; Yin et al. 2008; Zhang et al. 2003; Zhu et al. 2008). For example, Liu et al. (2007) reconstructed winter temperature variations since AD 1000 for the middle Qilian Mountains using *Sabina przewalskii*. Based on tree-ring samples from the same species, Gou et al. (2008) presented a maximum temperature reconstruction for the past 700 years in the Anymaqen Mountains area; On the southeastern TP, a summer temperature reconstruction since AD 1765 was established using tree-ring samples from *Abies georgei* var. *smithii* timberlines (Liang et al. 2009).

These climate reconstructions described climate history of several areas of the TP. However, the number of available tree-ring chronologies from the TP is still sparse.

Sabina tibetica, as one of the dominant species, has a wide distribution on the eastern TP, such as in the area of Yushu, Qamdo, and Linzhi. Tree-ring width of *S. tibetica* was found to be significantly correlated with the early summer climate (Bräuning 2001; Qin et al. 2003; Shi et al. 2010; Wang et al. 2008). In this paper, we present a temperature reconstruction based on a ring-width chronology of *S. tibetica* from Leiwuqi. The reconstruction should expand our knowledge of climate variability for this area.

2 Materials and methods

2.1 Study area

Our study area is located in Leiwuqi, Qamdo area of the eastern TP (Fig. 1). It is the source region of the Lancangjiang River. The climate of this area is controlled by the South Asian Monsoon in summer and by the southern branch of the westliers in winter. According to the meteorological record in Qamdo (97° 10′, 31° 9′, 3,307 m above sea level (a.s.l.); Fig. 2), July is the warmest month with a mean temperature of 16.4°C, and January the coldest (−2.19°C). Summer (June–August) precipitation (296 mm) accounts for 61.4% of the annual precipitation (482 mm). *S. tibetica* and *Picea likiangensis* var. *balfouriana* are the two dominant species in this area. In general, *S. tibetica* grows on the south-facing slope, while *Balfour spruce* on the north-facing slope.

2.2 Tree-ring sampling and chronology development

Tree-ring samples were bored from a well-drained, open-canopy, and south-facing *S. tibetica* forest at an elevation range from 3,967 to 4,042 ma.s.l. There is little evidence of disturbances due to fire or human activities. Twenty-five isolated trees were selected for sampling. Two (seldomly one) cores were taken for each tree at a height of about 0.70 m above ground. The tree-ring samples were glued, smoothed, and crossdated through traditional process of dendrochronology in the lab (Stokes and Smiley 1968). Then, we measured the ring width using Lintab with a resolution of 0.01-mm resolution. The Cofecha program (Holmes 1983) was used to check the quality of the crossdating and measurement.

Tree-ring chronology was developed using program Arstan (Cook 1985). We tried several methods of standardization on the raw ring-width data: 30, 80, 180, 230, 280, 330, 380 yearsr, 67% of series length smoothing spline, and negative exponential function or linear regression. The correlation between trees decreased with increasing first-order autocorrelation, suggesting the chronology signal weakened as more low-frequency variation was preserved in chronology. Accordingly, we finally used a 30-year smoothing spline with a 50% frequency cut-off to detrend each raw ring-width series to enhance growth variations on interannual to decadal timescales. The resulted index series

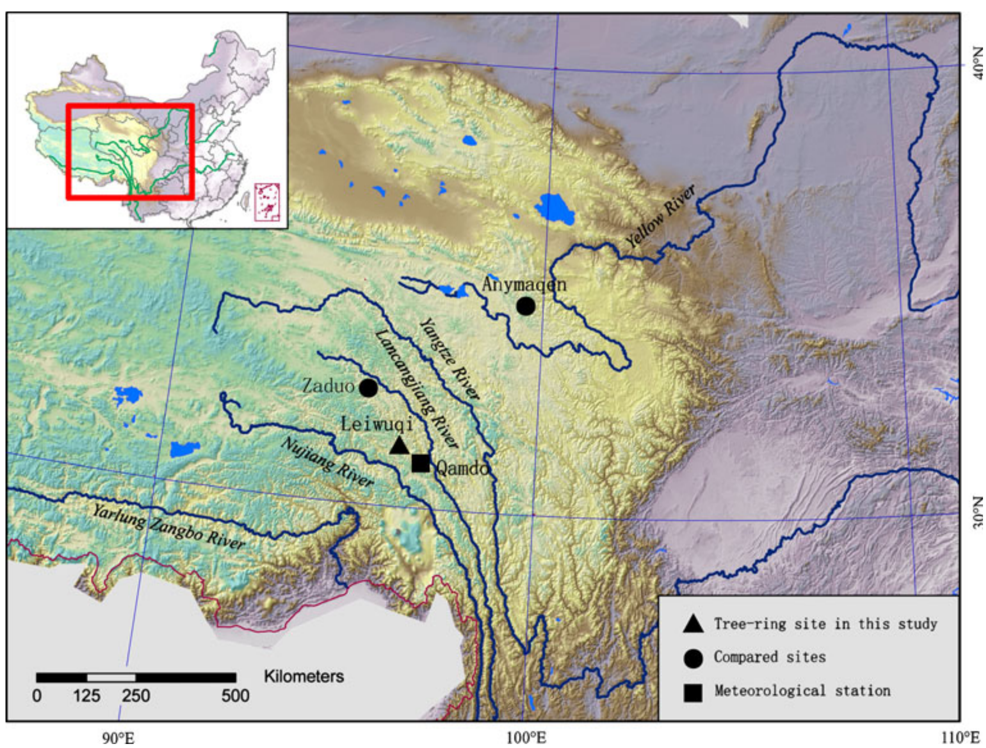

Fig. 1 Map showing tree-ring sampling sites, meteorological station, and compared sites in the text. Leiwuqi is the tree-ring sampling site in this study. Qamdo is the meteorological station. Zaduo (Shi et al. 2010) and Anymaqen (Gou et al. 2008) are the two compared tree-ring records

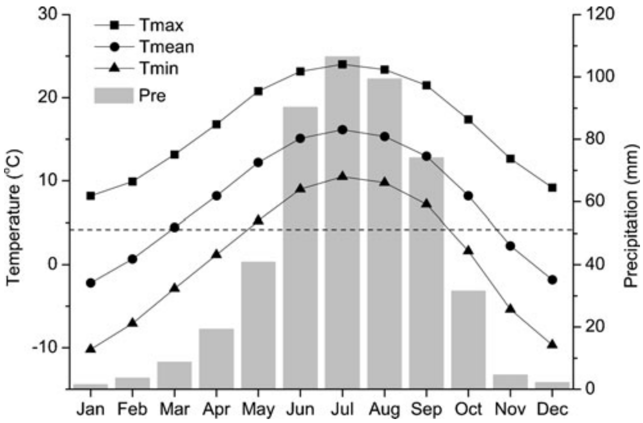

Fig. 2 Climate diagram from the meteorological station in Qamdo in the eastern Tibet Plateau from 1954 to 2007. The climate variables include the monthly maximum, mean and minimum temperatures, and monthly total precipitation (*bars*). The *horizontal dashed line* represents 0°C at 4,000 m with an adjustment of a lapse rate of −0.6°C/100 m from Qamdo meteorological station

were averaged bi-weightly into a chronology to diminish the influence of outliers. To quantify the signal strength among different indexed series, we conducted common interval analysis during 1800–2000. Several statistics were calculated, including variance explained by the first principal component (PC1), correlation between trees (BTR), correlation within trees (WTR), and expressed population signal (EPS) (Cook and Kairiukstis 1990). We also calculated running EPS every 50 years with a 25-year overlap to evaluate the representation of the chronology for population through time.

2.3 Tree growth-climate relationship and climate reconstruction

We correlated the ring-width chronology with monthly climate records from previous October to current September to investigate the tree growth-climate relationship. The climate variables included monthly mean/maximum/minimum temperatures and monthly total precipitation. The meteorological station in Leiwuqi (96° 36′, 31° 13′, 3,811 m) was the nearest one to the tree-ring sampling site. However, its record only started from 1991. Hence, we used the longer record (since 1954) from the Qamdo meteorological station, which is about 65 km southeast to the tree-ring sampling site. The temperature data of four seasons from Qamdo station had high correlations (the least one is 0.89 in summer) with those from Leiwuqi during 1991–2007. For precipitation, most correlations were higher than 0.84 except for the winter season (0.63).

We established several combinations of climate data for calculating correlation coefficients between the tree-ring chronology and climate variables. The seasonal variable having the highest correlation with the chronology was selected for the final reconstruction. The climate data were regressed against the ring-width chronology. The skill of the regression equation for the reconstruction back to AD 1440 was tested by cross-calibration/verification for the sub-periods 1954–1980 and 1981–2006, and by a leave-one-out cross-validation (LOOCV) (Michaelsen 1987) over the full-period 1954–2006. Evaluative statistics included the variance explained (R^2), the adjusted variance explained $\left(R^2_{adj}\right)$, the variance predicted (r^2), the sign test of both raw data and their first difference, the reduction of error (RE; Fritts 1976) and the coefficient of efficiency (CE; Briffa et al. 1988).

3 Results and discussion

3.1 Tree-ring chronology and statistics of the common interval analysis

Figure 3 shows the tree-ring-width chronology of *S. tibetica* from Leiwuqi. The chronology extended back to AD 1384, and could be considered reliable after AD 1440, when ten cores from six trees are available and EPS exceeds the recommended threshold of 0.85 (Wigley et al. 1984; Fig. 3). Both the variance explained by PC1 and the mean correlation BTR during 1800–2000 (Table 1) indicated high consistency between the different ring-width series.

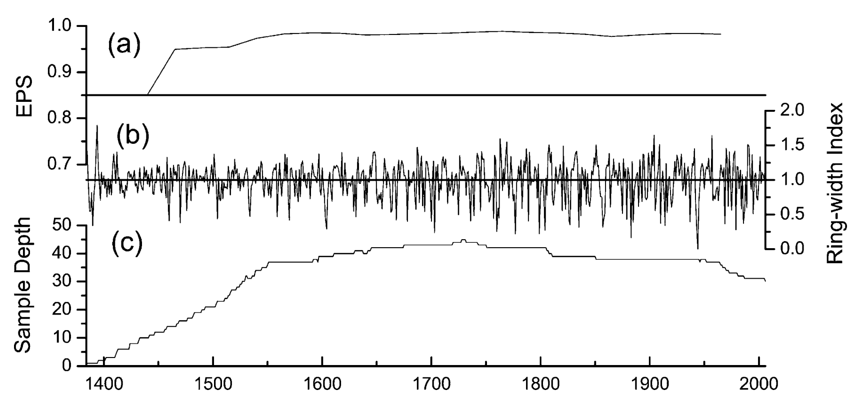

Fig. 3 Tree-ring width chronology of *Sabina tibetica* from Leiwuqi. **a** The 50-year running expressed population signal (EPS); **b** ring-width index of the chronology; **c** the sample depth of the chronology

Table 1 Site information of the tree-ring sampling site and the statistics in common interval analysis (1800–2000)

Site information	Latitude	Longitude	Altitude	MSL	Span	Trees/cores
	31.25° N	96.50°	3996 m	463	1384–2006	25/45
Common interval analysis	PC1	BTR	WTR	EPS	Span	Trees/cores
	0.59	0.57	0.59	0.98	1800–2000	18/30

MSL mean segment length, *PC1* explained variance of the first principal component, *BTR* correlation between trees, *WTR* correlation within trees, *EPS* expressed population signal

3.2 Relationships between chronology and climate data

The chronology showed negative correlations with temperatures from March to July and positive ones with precipitation from February to July (Fig. 4). The highest correlation between tree growth and temperature ($p<0.001$) were found for the seasonal window May–June. Seasonal precipitation also correlated significantly ($p<0.05$) with the chronology; however with lower correlation coefficients.

The negative correlations between tree growth and climate (Fig. 4) suggest that high temperature, particularly in May and June, limits the growth of *S. tibetica* in the eastern TP. This is in agreement with earlier studies (Bräuning 2001; Shi et al. 2010; Wang et al. 2008) on the same species from the eastern, central, and southwestern TP. Negative influences of early summer warmth on tree growth were reported for *S. przewalskii* on the northeastern TP (Gou et al. 2008; Liang et al. 2010; Liu et al. 2006; Shao et al. 2010; Sheppard et al. 2004; Zhang et al. 2003). In the western Himalayas, warm summers also limit the growth of *Juniperus polycarpos* (Yadav et al. 2010), *Cedrus deodara* (Yadav et al. 1997, 1999; Yadav et al. 2004) and *Abies pindrow* (Hughes 1992). In addition, Cai et al. (2008) found the limiting effect of May–Jun temperature on tree growth of *Pinus tabulaeformis* from the southeastern Chinese Loess Plateau. High temperature in early summer without sufficient precipitation increases transpiration and soil evaporation, and thus leads to strong moisture stress on tree growth (Cai et al. 2010; Gou et al. 2008; Yadav et al. 2010).

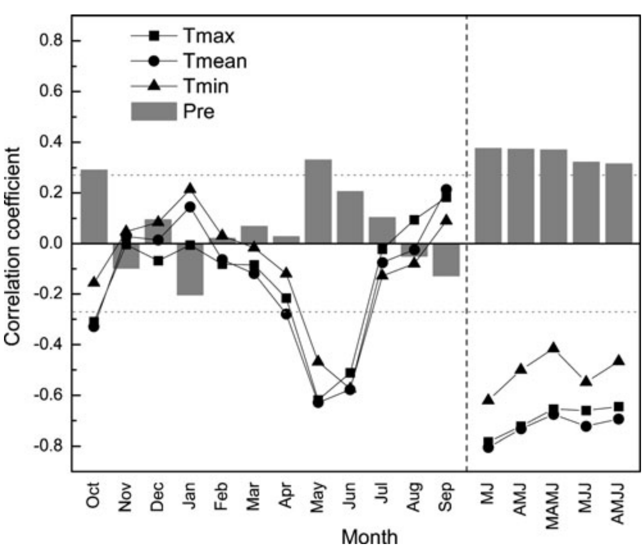

Fig. 4 Correlations between the ring-width chronology of *Sabina tibetica* and the mean monthly/seasonal climate variables from October of the pre-growth year to August of the current-growth year during 1954–2006. *Horizontal dotted lines* denote a significance level of $p=0.05$

3.3 Calibration/verification statistics and reconstructed temperatures

According to the correlations between tree-ring width and climate variables, we selected the May–June mean temperature for final reconstruction. The regression equations explained over 60% of the variance in the instrumental May–June temperature data, both in the calibration and verification periods (Table 2). Sign test showed that the estimated data were quite similar with the instrumental records. Both RE and CE indicated that the equations had good predictive skills for the mean May–June temperature. In addition, the regression coefficients were essentially the same for the two subperiods and the whole period. Finally, the equation during the whole period (1954–2006) was selected to reconstruct the mean May–June temperature variation back to AD 1440.

As shown in Fig. 5a, the reconstructed temperatures closely matched the instrumental record. However, our reconstruction might not capture low-frequency variations of May–June temperatures due to the application of the rigid 30-year spline in the standardization process of chronology construction. To ascertain the problem, we examined the 11-year smoothing curve of the instrumental and the estimated temperature data (Fig. 5a). The two curves show very similar decadal variations during 1954–2006. There are no significant autocorrelation ($r=-0.16$, Durbin–Watson$=2.00$) in the residuals between the instrumental and the estimated May–June temperature (Fig. 5b). In addition, the scatter plot clearly presented the linear relationship between the instrumental and estimated data (Fig. 5c). These analyses suggested that there should be no obvious loss of low-frequency variation in our reconstruction of May–June temperature at least during the instrumental period. Nevertheless, there may have occurred low-frequency temperature variations over the whole period

Table 2 The calibration and verification statistics for the May–June temperatures

Calibration period	1954–1980	1981–2006	1954–2006
Verification period	1981–2006	1954–1980	LOOCV[a]
Calibration			
R^2	0.682	0.603	0.641
$\left(R^2_{adj}\right)$	0.669	0.586	0.634
Verification			
r^2	0.603	0.675	0.613
RE	0.601	0.673	0.612
CE	0.596	0.669	
Sign test			
First difference	20+/5− **	22+/4−**	41+/11−**
Raw	20+/6− **	23+/4−**	42+/11−**
Regression weights			
a	15.6	15.7	15.7
b	−2.01	−2.05	−2.03

The regression equation is in the form of $y=a+bx$, where y denoted the mean May–June temperature, x equaled the value of the ring-width chronology, a and b are the constants

[a] LOOCV represents leave-one-out cross-validation (Michaelsen 1987)

**Stands for the significant level of 0.01

(1440–2006) that are not captured by our reconstruction due to the data treatment.

Figure 6 shows the reconstructed May–June temperature back to AD 1440 for Qamdo area. According to the 11-year moving average curve and their long-term (1440–2006) mean, warm periods could be identified during 1501–1514, 1528–1538, 1598–1609, 1624–1636, 1650–1668, 1695–1705, 1752–1762, 1794–1804, 1878–1890, 1909–1921, 1938–1949, and 1979–1991. Cool early summers occurred during 1440–1454, 1482–1500, 1515–1527, 1576–1597, 1610–1621, 1669–1679, 1706–1716, 1782–1793, 1863–1873, 1894–1908, and 1922–1937. The top five of the 28 high-temperature extremes (anomaly≥2 STD) were indicated in 1944, 1883, 1777, 1799, and 1460. The reconstruction showed only four cold extremes in 1904, 1957, 1763, and 1769. The lower number of cold extremes captured in the reconstruction may result from the finding that tree growth is more limited by higher temperatures.

We examined the spectral characteristics of our reconstruction using Multi-taper Method (Mann and Lees 1996). The reconstructed May–June temperature showed significant cycles at 23.8, 19.7, 13.0, 7.7, 5.1, 3.5, 2.6, 2.2 years (Fig. 7). Liang et al. (2008) also found a significant peak at 2.7 and 4.7 years in a summer temperature reconstruction for the Yushu area. The cycles of 23.8, 19.7, and 13.0 years are near the sunspot cycle of 11 years and its double.

3.4 Comparison with nearby temperature reconstructions

Our temperature reconstruction shows several warm/cold periods and extremes with other nearby temperature reconstructions. For example, the warm periods 1650–1668 and 1878–1890, and cool periods 1482–1500, 1610–1621, 1669–1679, 1706–716, 1762–1772, 1706–1716, 1894–1908, and 1922–1937 in our reconstruction are consistent with the Zaduo May–June maximum temperature reconstruction (Shi et al. 2010; Fig. 6). The warm periods 1624–1636, 1650–1668, and 1794–1804 are in good agreement with the March–May temperature reconstruction for the western Himalaya (Yadav et al. 1999). The western

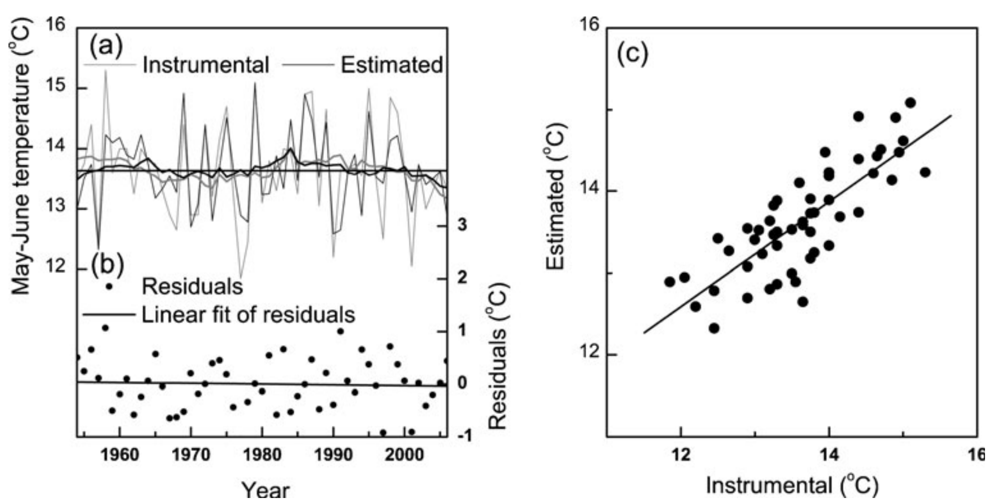

Fig. 5 Comparisons between the instrumental and estimated May–June temperature of Qamdo. **a** The instrumental and estimated May–June temperatures with their 11-year moving averages (the *thick solid lines*); **b** the residuals of the instrumental and estimated May–June temperatures; **c** the scatter plot of instrumental and estimated May–June temperatures

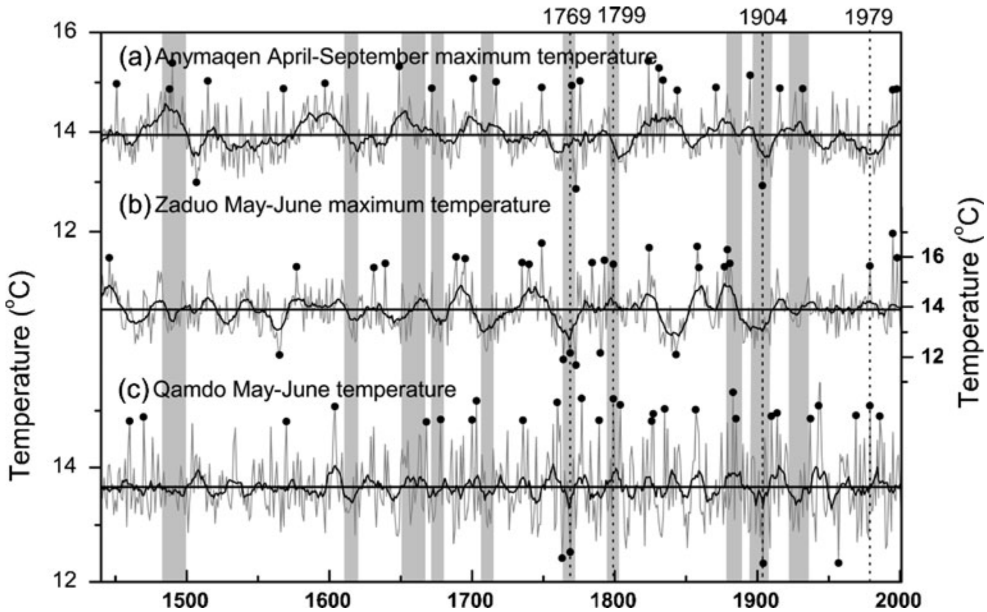

Fig. 6 Comparison between our temperature records with other reconstructions along the eastern margin of the Tibetan Plateau over the 1440–2001 period. **a** April–September maximum temperature reconstruction for the Anymaqen area (Gou et al. 2008); **b** the reconstructed Zaduo May–June maximum temperature (Shi et al. 2010); **c** our May–June temperature reconstruction for Qamdo. The *thick lines* represent their 11-year moving average. The *solid circles* are their high/low extremes (≥2 STD)

Himalayan record also shows cool conditions identified in our reconstruction during 1440–1454, 1515–1527, and 1922–1937 periods. A regional tree-ring width chronology of *S. tibetica* for the Qamdo area (Bräuning 2001), which had negative correlations with temperature from March to June of the growth year, indicated relatively higher growth rates during 1490–1500, 1570–1580, and 1780–1790 periods. These periods correspond to the cooler episodes in our reconstruction. In addition, our reconstruction shows common warm extremes in 1799 and 1979, cold one in 1769 with the Zaduo reconstruction (Shi et al. 2010). The cold extreme in 1904 identified in our reconstruction is also indicated to be extreme in the Anymaqen April–September maximum temperature reconstruction (Gou et al. 2008; Fig. 6). The agreement between our reconstruction and these nearby proxy records indicates that our reconstruction should be of good reliability.

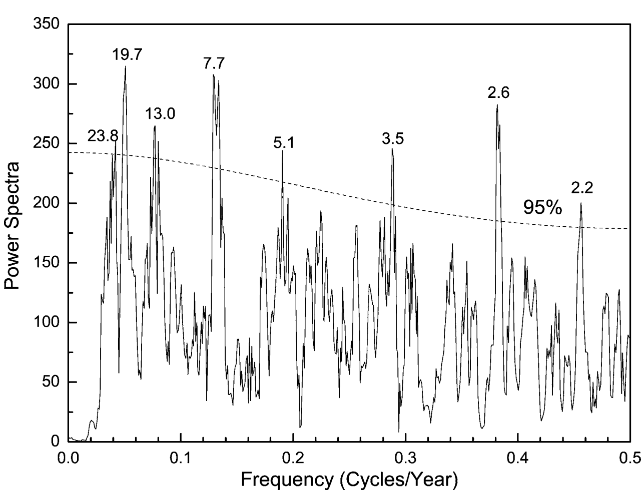

Fig. 7 Power spectra of the reconstructed May–June temperature for Qamdo during 1440–2006

In general, there is little agreement between our reconstruction and the Anymaqen April–September maximum temperature record (Gou et al. 2008; Fig. 6). They had opposite warm/cold variations during some periods, such as 1482–1550, 1794–1804, and 1922–1937. Spatial correlations between the Qamdo reconstruction and the Anymaqen record (Gou et al. 2008) with the corresponding CRU-gridded temperature dataset (Mitchell and Jones 2005) reveal their different geographical representation (Fig. 8a and c). The Qamdo reconstruction is associated with the temperature field south of approximately 34° N with a north–south extension along the moisture passage from the Bay of the Bengal (Fig. 8a). However, the temperature field of the Anymaqen reconstruction (Gou et al. 2008) is north to about 33–34°N with the core region in the Anymaqen Mountains area (Fig. 8c). The temperature fields of the proxy data are basically validated by the meteorological data, despite their relatively larger spatial representation (Fig. 8b, d). Further investigation of the synoptic circulation features using the

Fig. 8 Spatial correlations of temperature records with corresponding CRU-gridded temperature dataset (Mitchell and Jones 2005) over 1959–2001 and the synoptic circulation features. **a** and **b** are the correlation fields (with $p < 0.05$ filtered out) of the reconstructed and instrumental Qamdo May–June mean temperature, respectively (plotted using the Climate Explorer: http://climexp.knmi.nl); **c** and **d** are the correlation fields of the reconstructed and instrumental April–September maximum temperature for the Anymaqen area (Gou et al. 2008); **e** and **f** are the composite mean of NCEP (Kalnay et al. 1996) May–June geopotential height and vector wind at the 500 hpa during 1954–2006 (plotted using the PSD Interactive Plotting and Analysis Pages: http://www.esrl.noaa.gov)

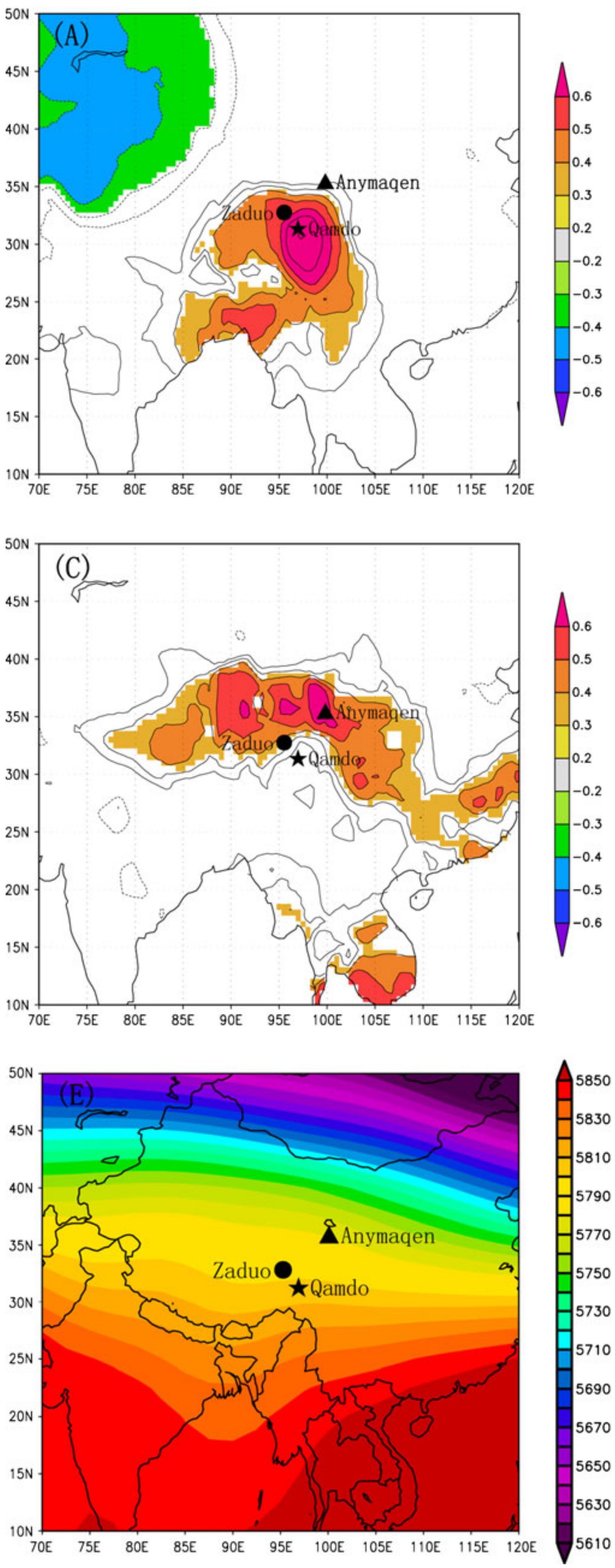
(A)
(B)
(C)
(D)
(E)
(F)
Anymaqen
Zaduo
Qamdo
50N
45N
40N
35N
30N
25N
20N
15N
10N
70E 75E 80E 85E 90E 95E 100E 105E 110E 115E 120E
0.6
0.5
0.4
0.3
0.2
−0.2
−0.3
−0.4
−0.5
−0.6
5850
5830
5810
5790
5770
5750
5730
5710
5690
5670
5650
5630
5610
12
11
10
9
8
7
6
5
4
3
2

500 hpa geopotential height from the NCEP reanalysis dataset (Kalnay et al. 1996) indicated that the climate of the Qamdo area and the Anymaqen area are influenced by different synoptic regimes. The Qamdo area is located at the eastern front of India–Burma trough (Wu and Zhang 1998) (Fig. 8e) during the May–June period, leading to dominant southwesterly flow (Fig. 8f). On the contrary, relatively fewer southwest flows can reach the Anymaqen area in May to June. The area is more influenced by northwesterlies.

4 Conclusion

In this paper, we presented a 567-year May–June temperature reconstruction for the Qamdo area based on a new tree-ring width chronology of *S. tibetica*. The reconstruction indicates that warm conditions occurred during 1501–1514, 1528–1538, 1598–1609, 1624–1636, 1650–1668, 1695–1705, 1752–1762, 1794–1804, 1878–1890, 1909–1921, 1938–1949, and 1979–1991. The Qamdo area experienced cool early summers during periods of 1440–1454, 1482–1500, 1515–1527, 1576–1597, 1610–1621, 1669–1679, 1706–1716, 1782–1793, 1863–1873, 1894–1908, and 1922–1937. Comparisons with other proxy records and meteorological record validate our reconstruction on both spatial and temporal scales. However, there is obvious spatial variability in the May–June temperature variations along the eastern margin of the TP. Since tree growth of *Sabina* trees on the TP shares coherently inverse relationship with early summer temperatures, there should be great potential to develop a tree-ring network for reconstruct spatial and temporal variability of early summer temperatures over the past few hundred years for this vast area.

Acknowledgments This work is supported by the National Natural Science Foundation of China (40801033 and 40871097) and the Knowledge Innovation Program of the Chinese Academy of Sciences (Grant No. KZCX2-YW-Q1-01 KZCX2-YW-QN111). We thank Prof. Xiaohua Gou for providing their reconstructed data for comparison in this study. Thanks were also given to the two anonymous referees and Editor Prof. Dr. Hartmut Graßl for their helpful and constructive suggestions and comments on the MS.

References

Bräuning A (2001) Climate history of the Tibetan Plateau during the last 1000 years derived from a network of Juniper chronologies. Dendrochronologia 19:127–137

Bräuning A, Mantwill B (2004) Summer temperature and summer monsoon history on the Tibetan plateau during the last 400 years recorded by tree rings. Geophys Res Lett 31 doi:10.1029/2004GL020793

Briffa KR, Jones PD, Pilcher JR, Hughes MK (1988) Reconstructing summer temperatures in northern Fennoscandinavia back to AD 1700 using tree-ring data from Scots pine. Arct Alp Res 20:385

Cai QF, Liu Y, Song HM, Sun JY (2008) Tree-ring-based reconstruction of the April to September mean temperature since 1826 AD for north-central Shaanxi Province, China. Sci China Ser D 51:1099–1106

Cai QF, Liu Y, Bao G, Lei Y, Sun B (2010) Tree-ring-based May–July mean temperature history for Lüliang Mountains, China, since 1836. Chin Sci Bull 55:3008–3014. doi:10.1007/s11434-11010-13235-z

Cook ER (1985) A time series analysis approach to tree ring standardization. University of Arizona, Tuscon, p 171

Cook ER, Kairiukstis LA (1990) Methods of dendrochronology: applications in the environmental sciences. Kluwer Academic Publishers, Dordrecht

Fritts HC (1976) Tree rings and climate. Academic, London

Gou XH, Peng JF, Chen FH, Yang MX, Levia DF, Li JB (2008) A dendrochronological analysis of maximum summer half-year temperature variations over the past 700 years on the norheastern Tibetan Plateau. Theor Appl Climatol. doi:10.1007/s00704-00007-00336-y

He HY, Mcginnis JW, Song ZS, Yanai M (1987) Onset of the Asian Summer Monsoon in 1979 and the effect of the Tibetan plateau. Mon Weather Rev 115:1966–1995

Holmes RL (1983) Computer-assisted quality control in tree-ring dating and measurement. Tree-Ring Bull 43:69–78

Hughes MK (1992) Dendroclimatic evidence from the western Himalaya. In: Bradley RS, Jones PD (eds) Climate Since AD 1500. Routledge Press, London, pp 415–431

Kalnay E, Kanamitsu M, Kistler R, Collins W, Deaven D, Gandin L, Iredell M, Saha S, White G, Woollen J, Zhu Y, Chelliah M, Ebisuzaki W, Higgins W, Janowiak J, Mo KC, Ropelewski C, Wang J, Leetmaa A, Reynolds R, Jenne R, Joseph D (1996) The NCEP/NCAR 40-year reanalysis project. Bull Am Meteorol Soc 77:437–471

Li CF, Yanai M (1996) The onset and interannual variability of the Asian summer monsoon in relation to land sea thermal contrast. J Climate 9:358–375

Liang EY, Eckstein D (2009) Dendrochronological potential of the alpine shrub Rhododendron nivale on the south-eastern Tibetan Plateau. Ann Bot 104:665–670

Liang EY, Shao XM, Qin NS (2008) Tree-ring based summer temperature reconstruction for the source region of the Yangtze River on the Tibetan Plateau. Glob Planet Change 61:313–320

Liang EY, Shao XM, Xu Y (2009) Tree-ring evidence of recent abnormal warming on the southeast Tibetan Plateau. Theor Appl Climatol 98:9–18

Liang E, Shao XM, Eckstein D, Liu XH (2010) Spatial variability of tree growth along a latitudinal transect in the Qilian Mountains, northeastern Tibetan Plateau. Can J For Res 40:200–211

Liu Y, An ZS, Ma HZ, Cai QF, Liu ZY, Kutzbach JK, Shi JF, Song HM, Sun JY, Yi L, Li Q, Yang YK, Wang L (2006) Precipitation variation in the northeastern Tibetan Plateau recorded by the tree rings since 850 AD and its relevance to the Northern Hemisphere temperature. Sci China Ser D 49:408–420

Liu X, Shao X, Zhao L, Qin D, Chen T, Ren J (2007) Dendroclimatic temperature record derived from tree-ring width and stable carbon isotope chronologies in the middle qilian mountains, China. Arct Antarct Alp Res 39:651–657

Mann ME, Lees JM (1996) Robust estimation of background noise and signal detection in climatic time series. Clim Change 33:409–445

Michaelsen J (1987) Cross-validation in statistical climate forecast models. J Clim Appl Meteorol 26:1589–1600

Mitchell TD, Jones PD (2005) An improved method of constructing a database of monthly climate observations and associated high-resolution grids. Int J Climatol 25:693–712

Qin NS, Shao XM, Jin LY, Wang QC, Zhu XD, Wang Z, Li JB (2003) Climate change over southern Qinghai Plateau in the past 500 years recorded in *Sabina tibetica* tree rings. Chin Sci Bull 48:2483–2487

Shao XM, Huang L, Liu HB, Liang EY, Fang XQ, Wang LL (2005) Reconstruction of precipitation variation from tree rings in recent 1000 years in Delingha, Qinghai. Sci China Ser D 48:939–949

Shao XM, Xu Y, Yin ZY, Liang EY, Zhu HF, Wang SZ (2010) Climatic implications of a 3585-year tree-ring width chronology from the northeastern Qinghai-Tibetan Plateau. Quat Sci Rev. doi:10.1016/j.quascirev.2010.1005.1005

Sheppard PR, Tarasov PE, Graumlich LJ, Heussner KU, Wagner M, Osterle H, Thompson LG (2004) Annual precipitation since 515 BC reconstructed from living and fossil juniper growth of northeastern Qinghai Province, China. Climate Dyn 23:869–881

Shi XH, Qin NS, Zhu HF, Shao XM, Wang QC, Zhu XD (2010) May–June mean maximum temperature change during 1360–2005 as reconstructed by tree of *Sabina tibetica* in Zaduo, Qinghai Province. Chin Sci Bull 55:3023–3029. doi:10.1007/s11434-11010-13237-x

Stokes MA, Smiley TL (1968) An introduction to tree ring dating. University of Chicago Press, Chicago

Wang XC, Zhang QB, Ma KP, Xiao SC (2008) A tree-ring record of 500-year dry-wet changes in northern Tibet, China. Holocene 18:579–588

Wang L, Duan J, Chen J, Huang L, Shao X (2009) Temperature reconstruction from tree-ring maximum density of Balfour spruce in eastern Tibet. China Int J Climatol. doi:10.1002/joc.2000

Wigley TML, Briffa KR, Jones PD (1984) On the average value of correlated time series, with applications in dendroclimatology and hydrometeorology. J Clim Appl Meteorol 23:201–213

Wu GX, Zhang YS (1998) Tibetan Plateau forcing and the timing of the monsoon onset over South Asia and the South China Sea. Mon Weather Rev 126:913–927

Yadav RR, Park WK, Bhattacharyya A (1997) Dendroclimatic reconstruction of April–May temperature fluctuations in the western Himalaya of India since AD 1698. Quat Res 48:187–191

Yadav RR, Park WK, Bhattacharyya A (1999) Spring-temperature variations in western Himalaya, India, as reconstructed from tree-rings: AD 1390–1987. Holocene 9:85–90

Yadav RR, Park WK, Singh J, Dubey B (2004) Do the western Himalayas defy global warming? Geophys Res Lett 31:L17201. doi:17210.11029/12004GL020201

Yadav RR, Bräuning A, Singh J (2010) Tree ring inferred summer temperature variations over the last millennium in western Himalaya, India. Clim Dyn. doi:10.1007/s00382-00009-00719-00380

Yang B, Kang XC, Bräuning A, Liu J, Qin C, Liu J (2009) A 622-year regional temperature history of southeast Tibet derived from tree rings. Holocene. doi:10.1177/0959683609350388

Yin ZY, Shao XM, Qin NS, Liang E (2008) Reconstruction of a 1436-year soil moisture and vegetation water use history based on tree-ring widths from Qilian junipers in northeastern Qaidam Basin, northwestern China. Int J Climatol 28:37–53

Zhang QB, Cheng GD, Yao TD, Kang XC, Huang JG (2003) A 2, 326-year tree-ring record of climate variability on the northeastern Qinghai-Tibetan Plateau. Geophys Res Lett 30:1739–1741

Zhou XJ, Zhao P, Chen JM, Chen LX, Li WL (2009) Impacts of thermodynamic processes over the Tibetan Plateau on the Northern Hemispheric climate. Sci China Ser D 52:1679–1693

Zhu HF, Zheng YH, Shao XM, Liu XH, Xu Y, Liang EY (2008) Millennial temperature reconstruction based on tree-ring widths of Qilian juniper from Wulan, Qinghai Province, China. Chin Sci Bull 53:3914–3920